Elastic and inelastic angular distributions of the $^{7}Li+^{120}Sn$ system for energies near the Coulomb barrier

2016 J. Phys. G: Nucl. Part. Phys. 43 055103

(http://iopscience.iop.org/0954-3899/43/5/055103)

IOP Publishing Journal of Physics G: Nuclear and Particle Physics

J. Phys. G: Nucl. Part. Phys. **43** (2016) 055103 (13pp) doi:10.1088/0954-3899/43/5/055103

Elastic and inelastic angular distributions of the ^{7}Li+^{120}Sn system for energies near the Coulomb barrier

V A B Zagatto[1,2], J R B Oliveira[1], L R Gasques[1,3], J A Alcántara-Núñez[1], J G Duarte[1,3], V P Aguiar[1], N H Medina[1], W A Seale[1], K C C Pires[1], A Freitas[1], J Lubian[4], J M B Shorto[5], F A Genezini[5] and E S Rossi Jr[6]

[1] Instituto de Fısica da Universidade de São Paulo, Brazil
[2] Istituto Nazionali di Fısica Nucleare—Laboratori Nazionali del Sud, Italy
[3] Istituto Nazionali di Fısica Nucleare—Sezione di Napoli and Dipartimento di Matematica e Fisica Seconda Universitá degli Studi di Napoli, Italy
[4] Instituto de Fısica da Universidade Federal Fluminense, Brazil
[5] Instituto de Pesquisas Energéticas e Nucleares, Brazil
[6] Centro Universitário FIEO—UNIFIEO, Brazil

E-mail: vinicius.zagatto@gmail.com

Received 21 January 2016
Accepted for publication 10 February 2016
Published 5 April 2016

Abstract

The reaction of ^{7}Li+^{120}Sn has been measured at bombarding energies of 21, 24 and 27 MeV. The $2^{+} \rightarrow 0^{+}$ γ-ray transition in ^{120}Sn was observed and the angular distribution for the 2^{+} excited state was obtained. Coupled channels and coupled-reaction channels calculations, including the dynamical polarization potential due to the projectile break-up, obtained from continuum discretized coupled channel calculations, were performed. The comparison between the existing experimental elastic angular distribution with the coupled-reaction channels calculations indicates that the 1n stripping transfer is the most intense channel to be coupled and the 2n stripping reaction occurs sequentially rather than directly, however, further data must be analyzed to confirm this indication. The experimental elastic and inelastic scattering data were well described by the calculations, but some discrepancies in these channels may indicate the need for corrections to the nuclear potential and/or the necessity to incorporate further channels.

Keywords: inelastic scattering, break-up, γ-particle coincidence, γ-ray spectrometer

(Some figures may appear in colour only in the online journal)

1. Introduction

The understanding of nuclear reactions involving weakly bound stable and unstable nuclei is important, not only in itself, but also for other research fields such as astrophysics. Primordial nucleosynthesis, supernova nucleosynthesis, energy generation in stars, and other astrophysical scenarios involve reactions in which such nuclei participate in a determinant way. Information about the cross sections of the processes involved is fundamental to the knowledge of the reaction rates and, consequently, for the understanding of astrophysical evolution and, ultimately, the history of the universe. In many cases, the extreme conditions of the environment, such as very low energies, participation of nuclei very far from the stability line, etc, can prevent a direct measurement of the relevant quantities involved. In such cases, only by extrapolation from more easily accessible regions is it possible to infer the necessary information. For these extrapolations to be reliable, a very good understanding of the relevant physical processes involved is required to guide the extrapolations and provide reliability to the predictions. One of these processes is the break-up phenomenon which contributes significantly in the weakly bound system reactions. This phenomenon is still not completely understood, even with stable nuclei. Other features, such as the form of the optical potential and the coupling strengths to various reaction channels are important for a better understanding of reaction mechanisms.

A detailed understanding of reactions with radioactive nuclei can only be expected after a proper understanding of the stable systems. As the intensity of stable beams is presently much higher than that which can be obtained with the radioactive ones, it is still interesting to make experiments with stable beams, because a much larger statistical significance and improved measurement precision can be achieved, allowing for the investigation of detailed aspects of the reaction mechanisms.

In this work, we study the reaction of the weakly bound stable beam of ^{7}Li on a ^{120}Sn target. The Saci-Perere γ-ray spectrometer [1] (originally developed for nuclear structure studies) has been adapted to study nuclear reaction mechanisms by the particle-γ coincidence technique [2]. Reactions involving these nuclei have already been measured separately in other experiments, such as ^{7}Li $+^{144}$Sm [3], ^{7}Li $+^{65}$Cu [4], and ^{6}Li $+^{120}$Sn [5]. For the ^{7}Li $+^{120}$Sn system, the elastic scattering angular distributions have been measured at a few beam energies [5–7].

Reference [5] also reports inelastic measurements for this reaction, however, for energies much above the Coulomb barrier. The particle-γ technique, taking advantage of the high energy resolution of HPGe γ-ray detectors, allows for the identification and measurement of the inelastic excitation of the 2^{+} state of ^{120}Sn, among other processes such as particle transfer, complete and incomplete fusion. It has been reported that the break-up of ^{7}Li is sometimes preceded by particle transfer [8–10]. The identification and measurement of these processes is therefore important for the complete understanding of the reaction mechanisms. Data on these channels will be reported in future publications.

One of the main objectives of this work is to measure the inelastic scattering angular distribution of the 2^{+} state of ^{120}Sn for several ^{7}Li beam energies. Furthermore, the effects of coupling transfer partitions to elastic and inelastic channels are also studied, helping to understand if the discrepancies between experimental data and theoretical calculations are due to the coupling of channels or for the need of corrections to the nuclear potential.

In the next section, the description of the experimental setup is presented. The experimental method and data analysis are described in section 3, and the theoretical calculations in section 4. The theoretical and experimental results for the elastic and inelastic channels together with their discussion are presented in section 5, followed by the conclusions.

Figure 1. Exploded view of the truncated rings which compose the collimating set used in the experiment.

Table 1. Particle detectors and respective collimator settings. The polar and azimuthal (θ and ϕ) central angles relative to the beam direction and opening ranges are shown.

Detector	$\bar{\theta}$	$\bar{\varphi}$	$\Delta\theta$	$\Delta\phi$
1	28.4°	180°	4.1°	60°
2 and 3	42.7°	36°	6.1°	120°
4	54.4°	144°	6.7°	67°
5	66.6°	216°	6.0°	66°
6	78.7°	288°	6.7°	53°
7	104.0°	324°	6.5°	53°
8	113.4°	36°	6.0°	66°
9 and 10	142.5°	216°	5.0°	120°

2. Experimental setup

The ^{7}Li beam was accelerated by the Pelletron 8UD Tandem facility, at the Instituto de Fısica at the Universidade de São Paulo with intensities of about 3-15 nA at bombarding energies of 18, 21, 24 and 27 MeV in the laboratory frame. The ^{7}Li beam was extracted from the ion source using a lithium hydroxide cathode. The target consisted of a ^{120}Sn (>99% isotopic enrichment) self-supporting foil with a thickness of 1.66 mg cm^{-2}.

The Saci-Perere γ-ray spectrometer used in this work consists of four Compton suppressed HPGe $\gamma-$ray detectors (two of 60% and two of 20% efficiency relative to a $3' \times 3'$ NaI(Tl) scintillator detector) and eleven $\Delta E - E$ plastic phoswich scintillators for charged particle measurements [1]. In the present experiment, one of the 20% HPGe detectors and one of the phoswich scintillators were not operational. The setup was similar to that reported in [2], but the charged particle collimator system inside the scattering chamber was redesigned for the present experiment and consists of truncated Al rings with varying diameters (figure 1).

The scattering angles were limited by the gaps between the rings. Table 1 presents the central and aperture angles of each gap. The pairs of detectors 2 and 3, and 9 and 10, set at the same average polar angle were analyzed together as a single data point. A thick (about 1mm) ^{181}Ta disk was used as the beam stopper at the end of a small Faraday cup inside the chamber. The polar and azimuthal angles (θ, φ) of the $\gamma-$ray detector axes, with respect to the beam direction, were (101°, 0°) and (37°, 180°), for the 60% detectors, and (37°, 144°) for the 20% detector.

The electronic system was similar to those reported in [1, 2]. The event trigger was generated by a coincidence of the timing pulses of any one of the HPGe detectors with any one of the particle detectors within a ~500 ns time window. Besides the charged particle and γ-ray energy information of each detector, the event also contains the time difference between each γ-ray detector and the first particle detector pulse. For further details, see [11].

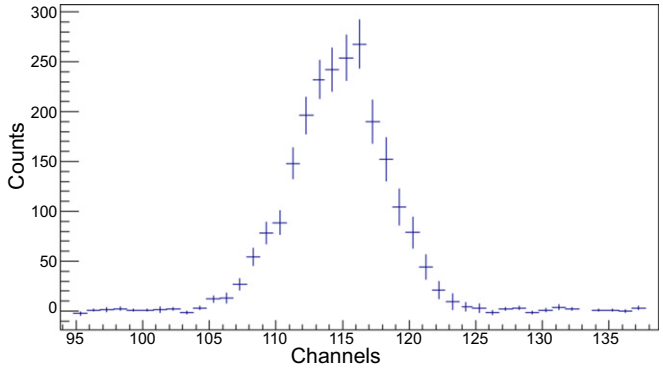

Figure 2. Particle energy spectrum of Z = 3 particles detected at ($\bar{\theta}_p = 67°$) in coincidence with the $2^+ \rightarrow 0^+$ 1171 keV γ transition from the ^{120}Sn target at $\theta_\gamma = 101°$.

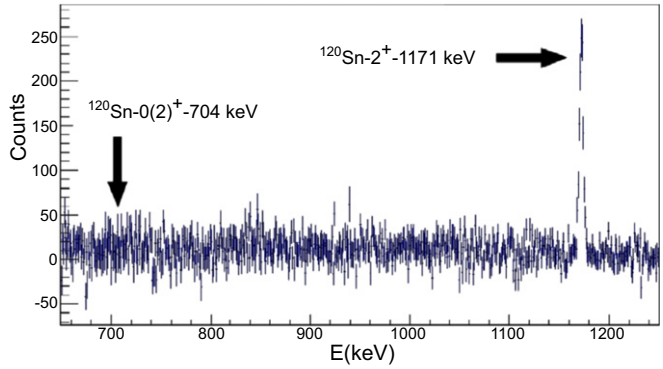

Figure 3. γ-ray energy spectrum at $\theta_\gamma = 101°$ in coincidence with $Z = 3$ charged particles detected at $\bar{\theta}_p = 43°$ to the beam direction (laboratory frame), showing the transition from the 2^+ inelastic excitation of the target. The position expected for the peak from the $0^+(2)$ excited state (with negligible cross section) is also shown.

3. Experimental method and data analysis

Details of the method and equations employed in data reduction of inelastic angular distributions are reported in [2]. For inelastic scattering, the peak areas of each particle detector are normalized with respect to the data at a sufficiently forward angle, and at each angle, in its turn, are normalized with respect to the reference data at a sufficiently low beam energy so that the theoretical cross section calculations are considered reliable at the reference data points. This procedure minimizes systematic errors, such as small offsets in detection angle, uncertainty in the detection solid angle, beam intensity variation, dead time correction, γ detection efficiency, and uncertainty in target thickness.

The reference measurement for normalization was performed at a beam energy of 18 MeV (below the barrier: $E_{\rm bar} = 21.4$ MeV). Theoretical corrections relative to a pure Coulomb excitation were included in the normalization cross sections to improve accuracy. The reference normalization angle for the present experiment was chosen to be 54.4°. At this angle

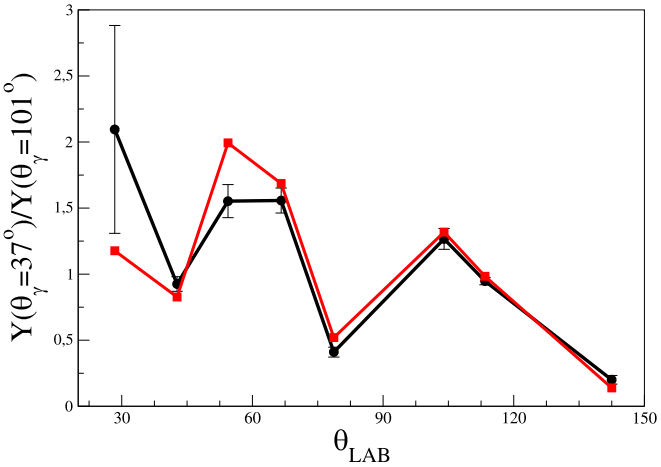

Figure 4. Experimental yield ratios between γ detectors at $\theta_\gamma = 37°$ and $\theta_\gamma = 101°$ (relative to the beam direction), at a beam energy of 24 MeV, as a function of the particle detector polar angle ($\bar{\theta}_{\mathrm{LAB}}$). The red squares (joined by straight lines to guide the eye) are the predicted ratios obtained from the theoretical calculations. The experimental yield ratios are the black data points with error bars.

the inelastic cross section is suficiently large to result in signficant statistics for the normalization data point. This angle is still small enough for the theoretical calculations to be reliable.

Figure 2 shows, as a sample, a typical particle energy spectrum. This particular spectrum is of detector 5 ($\bar{\theta}_p = 67°$) gated by the $2^+ \rightarrow 0^+$ 1171 keV γ transition of ^{120}Sn at $\theta_\gamma = 101°$. Figure 3 presents a sample γ spectrum at $\theta_\gamma = 101°$ gated by particle detector 3 (at $\bar{\theta}_p = 43°$). Both spectra were obtained at 24 MeV beam energy.

Since the γ decay can be very anisotropic, angular correlation corrections must be applied to the data. In order to check the reliability of the calculations used in the γ-particle angular correlation corrections, the ratios of yields between γ detectors at different angles is plotted as a function of the particle detector polar angle and compared to the theoretical predictions (as described in [2]). The results are presented in figure 4. Note that the azimuthal angle differences between γ and particle detectors ($\varphi_\gamma - \varphi_p$, not shown in the figure) vary considerably and irregularly from point to point, as a function of the polar angle, and therefore a smooth curve is not to be expected. As can be observed, the differences between the calculations and experimental results are attributable to the experimental uncertainties. This is a necessary check to corroborate that the model calculations of the γ-particle angular correlations are consistent with the data, and is considered part of the analysis procedure, as explained in [2].

4. Theoretical calculations

The theoretical calculations performed in this work used the coupled channels code FRESCO [12]. Calculations considering only the inelastic states in view of coupled channels formalism were performed and, from now on, are called CC. The transfer channels were treated in the coupled reaction channels (CRC) formalism [12]. In order to take into account the break up of the weakly bound projectile ^{7}Li, the continuum discretized coupled channels (CDCC, see

[13]) technique was employed. As the coupling to the continuum demands a high computational capacity, a complete calculation including not only the continuum but also the bound states of inelastic and transfer channels becomes prohibitive. Therefore, the calculations were performed in two steps. In the first step, only the break-up of the projectile was calculated by the CDCC calculations. From these calculations, the trivially equivalent local polarization potential (TELP), also referred as PP [14], was obtained. In the second step, standard CC and CRC calculations containing the direct reaction channels including the PP obtained in the first step were performed. In this way, effects of the break-up on the other channels can, approximately, be taken into account. An internal imaginary potential (with a Woods–Saxon shape) was also included in the calculations in order to account for absorption channels such as complete and incomplete fusion.

The CDCC calculations considered only the break-up of ^{7}Li into an α particle plus a triton. No other break-up channels were included in the calculations, such as ^{6}Li plus a neutron, or the subsequent decay of the triton.

The CDCC calculations included the couplings among continuum states, continuum to bound states and also among bound states of ^{7}Li. Convergence of the calculations was achieved with 200 partial waves and a matching radius of 400 fm.

The other integration values (maximum bin radius, maximum multipole order of the expansion of the interaction optical potentials, etc) and bin parameters (bin width, maximum bin energy, maximum relative α-tritium angular momentum) converged to the same values reported in reference [13], and the details can be found there. The α-target and tritium-target optical potentials used in calculations were the ones used in reference [13] and taken from reference [15]. The potential that generates the bins (α-tritium interaction) was taken from reference [16]. This potential was shown to be able to describe well the position of ^{7}Li resonances as well as their width [13]. Quadrupole moment reorientation of the states was also considered. In this first step of the calculations, target excitations were not included to avoid double counting, as those were included in the second step, while the excited states of the projectile were included only in the first step for the same reason.

In the second step of the calculations, the channels which were chosen to be included had to follow two criteria: that the Q value of the reaction should not be too negative (implying low formation probability) nor too positive, so that the nuclei formed would evaporate particles before γ-ray emission. The appropriate theoretical description of the second situation is an open question in this field because it requires the coupling of the initial channel with the unbound states of the very excited nucleus that is formed after the transfer process (in the case that the binding energy of the transferred particles is high). We will not attempt to develop such a description in the present work.

The excitation energy after the transfer process was estimated from the optimum Q value as proposed in [17, 18]. After the already mentioned selection, four processes were coupled to the elastic in the final calculations: inelastic (couplings to the three first states of ^{120}Sn), proton pick-up (three lowest states of ^{119}In), one-neutron stripping (six lowest states of ^{121}Sn), and two-neutron stripping (eleven lowest states of ^{122}Sn). All the coupled states for each partition of this second input, and the transitions made in CRC calculations (double-ended arrows to indicate that the channels mutually affect each other up to infinite orders) are presented in figure 5. Concerning the number of inelastic states coupled in the first partition, it is important to note that, as shown by figure 3, the γ ray from the second excited state (third state of ^{120}Sn) is absent in experimental data. This fact is confirmed by theoretical calculations that indicate cross sections of the order of 10^{-4} mb for this state.

In the second part of the calculations, a matching radius of 30 fm is used, which is much less than that of the CDCC calculations, as inelastic and transfer reactions occur at near

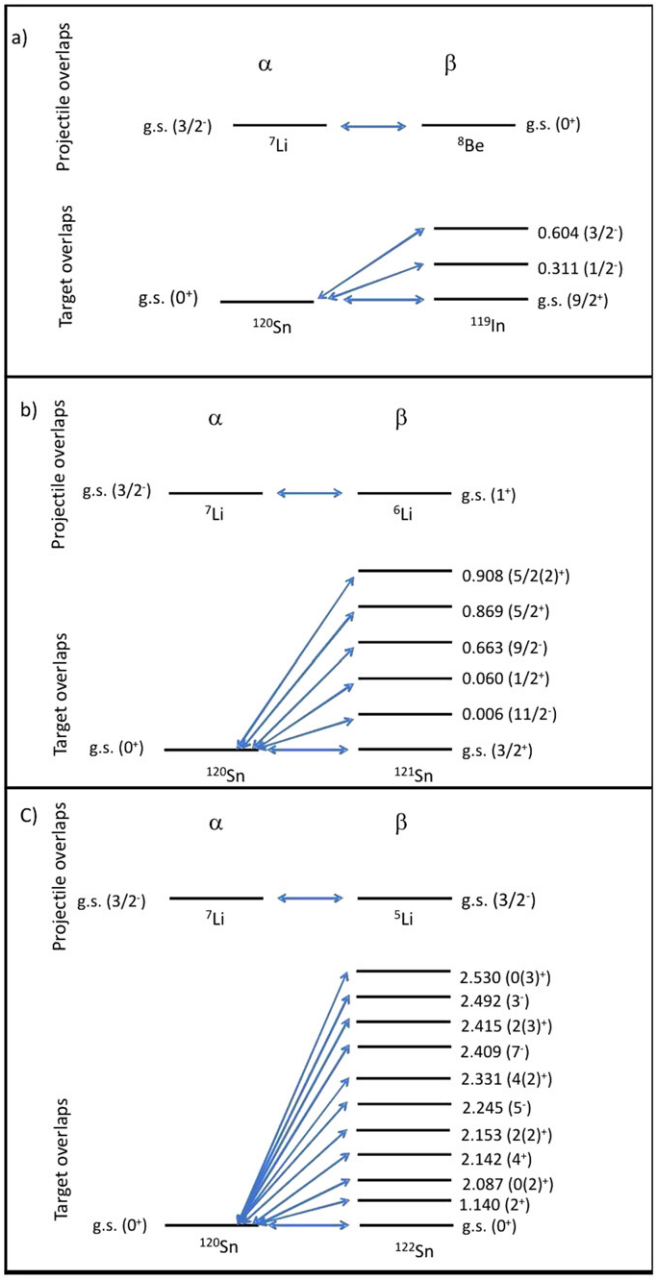

Figure 5. Schematic figure of the channels coupled in each partition and their respective transitions for diffent calculations. (a) One proton pick-up transfer, (b) one neutron stripping transfer, (c) two neutron stripping transfer for direct CRC calculation.

surface distances. The calculation was performed with orbital angular momenta from 0 to 90 $\hbar$ in this step. Again, the values used for the matching radius and for the maximum orbital angular momentum were those obtained after the convergence of the calculations was

achieved (higher values of both variables do not change significantly the angular distributions). The deformations of the potential of the first two excited states of ^{120}Sn were calculated as proposed by [19], using the experimental reduced transition probabilities from [20]. Quadrupole reorientation matrix elements were also obtained by the same procedure.

The optical potential of the initial partition was composed of the Coulomb interaction, the São Paulo potential (SPP) [21–23] with a normalization factor of 1.0 for the real nuclear part, an internal imaginary potential (Woods–Saxon shape with low difusivity), plus the TELP obtained in the first step.

The final transfer partitions optical potentials were composed of the Coulomb interaction plus a SPP nuclear interaction with normalizations of 1 and 0.78 for the real and imaginary parts, respectively, as proposed by SPP systematics [21–23]. The potentials between each core and valence particle (necessary to generate the single particle wave functions in cluster model) were composed of the Coulomb interaction plus a Woods–Saxon nuclear interaction (reduced radius of 1.2 fm and diffuseness of 0.6 fm) and a spin-orbit term. The core-core interactions were composed once again as proposed by SPP systematics.

In order to have control of the calculations performed, the different transfer partitions were coupled one at a time, observing the effect produced by this new coupling in the previous cross sections. The couplings of the inelastic channel and the one proton pick-up transfer channel produced almost no change to the elastic scattering. As the coupling of the one neutron stripping reaction was the first one to produce observable effects in the elastic scattering, the CRC calculations which contain all these previous channels (the one proton pick-up, the inelastic and the one neutron stripping channels) will be, now on, called CRC-1n, just for simplicity and to emphasize that this is the channel that is modifying the elastic scattering.

The two-neutron stripping can possibly occur by two different processes: direct transfer of a 2n cluster, or sequential transfer of two neutrons, through intermediate states in ^{121}Sn. The first case (direct) can be calculated by CRC assuming the transfer of a $J^{\pi} = 0^{+}$ dineutron cluster (therefore with no valence-core spin-orbit coupling). This calculation, which contains also all the previously mentioned partitions will be named CRC-2n Dir. from now on. In the second case (sequential) a negligible effect is expected onto the elastic and inelastic channels (the ones presently investigated), since the coupling of the 2n channel by sequential transfer of 2 neutrons cannot affect these channels, at least in a 2-step DWBA approximation [24]. Therefore, if the 2n transfer is of a sequential nature, the CRC-1n calculation already provides the best prediction we have for the elastic and inelastic channels. When any calculation presents the TELP included in it, the suffix PP will also be included to its name.

The nonlocal kernels for single particle finite range transfers were calculated with a nonlocality radius of 2.8fm (value required for the 2n transfer process). The transfer channels were calculated using prior representation with a complex remnant.

5. Results and discussion

5.1. Elastic scattering angular distributions

Figure 6 presents the calculated elastic angular distributions at the reference energy (18 MeV), and at 20.5 and 25 MeV in comparison to the data from [6]. The calculations were performed assuming the following models: pure Coulomb potential (Coul. Ex.), CC (including the nuclear optical potential and coupling to inelastic channels only), CC+PP, CRC-1n, CRC-1n +PP and CRC-2n Dir.+PP (these last three adding the respective transfer couplings to the CC +PP partition).

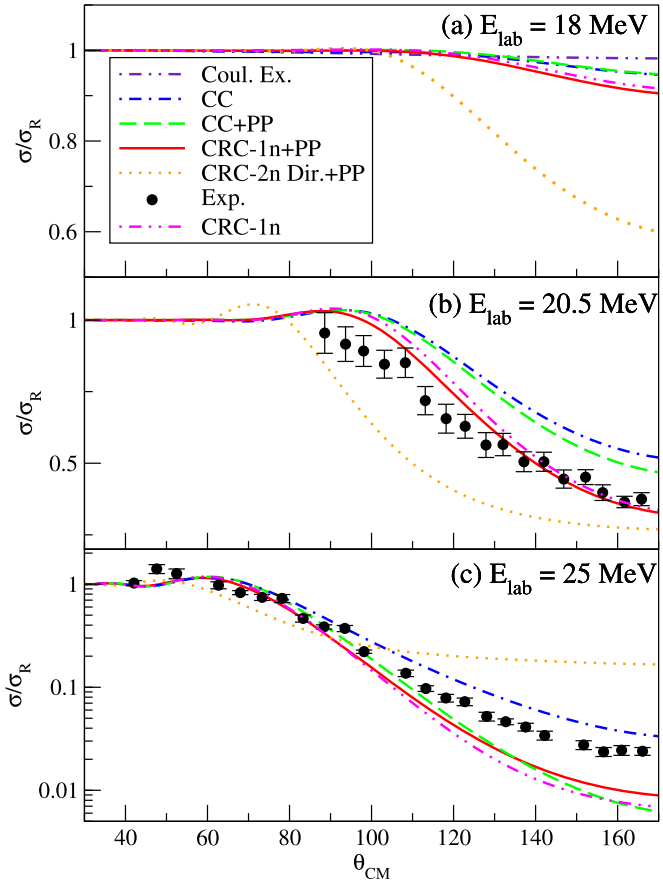

Figure 6. Elastic scattering angular distributions for the ^{7}Li +^{120}Sn reaction at a bombarding energy of (a) 18 MeV, (b) 20.5 MeV, and (c) 25 MeV. The lines of each type correspond to the model calculations described in the text, as identified in the inset in (a). The experimental data points (Exp.) presented in (b) and (c) are from [6]. The figures (b) and (c) do not contain the pure Coulomb excitation calculation curves.

As can be seen in figure 6(a), there are very small corrections for CC and CC+PP calculations to the pure Coulomb potential (including Coulomb excitation) at back angles (increasing from about 120° and up to, at most, a 1% magnitude). However, for CRC-2n Dir. calculation, these corrections become larger even at such a low beam energy, being almost 40% for this case. For CRC-1n calculations, the cross sections corrections are larger than those obtained by CC calculations, however, still much smaller than those obtained the CRC-2n Dir. one, being less than 10% difference when compared to the pure Coulomb potential.

Figure 6(b) shows the above calculations for a 20.5 MeV bombarding energy. The calculation for the 2n direct stripping process was performed with a 2n cluster spectroscopic factor of 0.7. This same value was adopted for the 1n transfer partition. There is an effect of decreasing the magnitude of the differential cross section (compared to CC calculations) as the transfer channels are coupled. The CRC-2n Dir.+PP calculations deviate from the data. The CRC-1n calculation is the one that best fits the data at 20.5 MeV, and, at 18 MeV, was the one used for normalization of the inelastic data.

Figures 6(b) and (c) indicate that the 2n direct transfer mechanism is inconsistent with the available data. With the direct 2n transfer assumption, no value in the interval from 0.5 to 1.5 for the cluster spectroscopic factor could fit the data properly. In the ^{7}Li extreme cluster model, the expected spectroscopic factor for the direct 2n transfer should be 1. Theoretically, a very small spectroscopic factor value is indeed to be expected, since both the dineutron and the corresponding core (^{5}Li) are very unstable, and such partition should have a very small contribution to the ^{7}Li ground-state wave function. In view of these results, we suggest that the direct extreme cluster model is a non realistic approximation for describing the ^{7}Li. The performed calculations indicate that the study of the behavior of the elastic cross section can help to elucidate if a transfer process occurs sequentially or directly, but a definitive answer is only possible after checking the transfer data itself, comparing it to the direct and sequential (2-step DWBA) calculations in order to determine which process is occurring. The data related to the 2n transfer channel is still under analysis. These data need more time to be properly evaluated since they involve the unstable nucleus ^{5}Li, which decays in an α particle and a proton, turning the analysis much more difficult.

From figure 6(b) (energy around the Coulomb barrier) it is possible to see that the effect of coupling transfer channels affect more significantly the elastic scattering than the inclusion of the PP, as suggests the comparison of CRC-1n with CC calculations.

From figure 6 it is possible to see that the effect of coupling the break-up to calculations (by comparing CC to CC+PP calculations or CRC-1n+PP to CRC-1n) increases as the bombarding energy also increases.

This result is in agreement with the conclusions reported in [3, 4, 8–10], where a high intensity one-neutron transfer channel was observed with a ^{7}Li projectile and triggered other two-step reactions.

5.2. Inelastic scattering angular distributions

The inelastic angular distributions corresponding to the excitation of the 2^{+} state of the target at 1.17 MeV excitation energy are presented in figure 7. The same model calculations as listed in the previous section were performed. In order to facilitate the comparison with the theoretical double differential cross section, the experimental data were renormalized by finite-to-pointlike factors ξ (so that the double differential cross section is related to the experimental yield Y by: $\frac{\mathrm{d}^2\sigma}{\mathrm{d}\Omega_p \mathrm{d}\Omega_\gamma} = \xi \frac{Y}{\Delta\Omega_p \Delta\Omega_\gamma}$). These factors were obtained theoretically through the calculation of the expected integrated yield both in the beam energy range (due to the finite target thickness) and the finite solid angle of the detectors ($\Delta\Omega_{p,\gamma}$) using the best (most reliable and accurate) theoretical model and parametrization (the CRC-1n+PP, in this case). Statistically, this procedure is equivalent to comparing the raw data with a theoretically based simulation, but presents more clearly the most physically meaningful quantities. One should be aware, though, that there may be some model related systematic error involved in the experimental data points. Note that the normalization procedure partly reduces the systematic errors originated from this factor, since the evaluation of the cross sections always involves yield ratios.

Comparing the CC+PP with the pure Coulomb excitation (Coul. Ex.) one can see, as expected, that the nuclear potential significantly reduces the large angle cross sections. This reduction starts at smaller angle and is more intense as the beam energy is increased. Apart from this major feature, the other couplings (transfers) have little influence on the angular distribution, except the 2n direct transfer which, when coupled, deviates somewhat from the other curves and from the data. This is another indication that the 2n transfer is probably

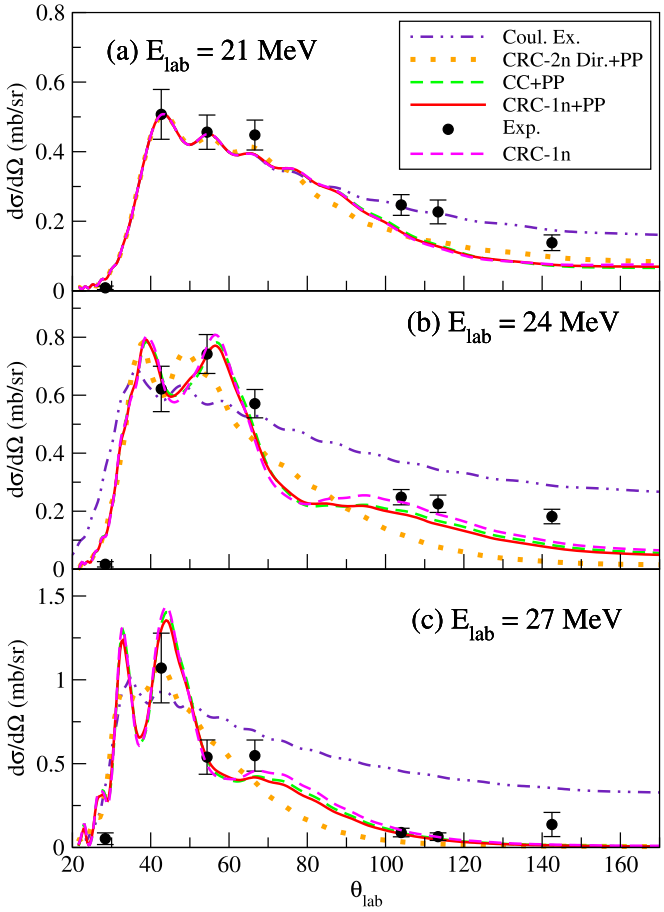

Figure 7. Angular distributions for the 2^+ state ar 1.17 MeV excitation of ^{120}Sn at (a) 21, (b) 24, and (c) 27 MeV. The experimental data obtained in the present work (black circles, with error bars) are presented. The lines of each type correspond to the model calculations described in the text, as identified in the inset in (a).

sequential. It is important to note that the discrepancies between the Coulomb Exc., CC+PP and CRC (any of them) calculations occur above the normalization point at 54.4°.

Through analysis of figure 7, one may see that the effect of coupling channels only decreases the cross section at back angles for energies above the Coulomb barrier. This can be observed in the 24 MeV data when comparing CC+PP to CRC calculations. At 21 MeV the discrepancy between these calculations and experimental data may indicate that the nuclear potential is slightly overestimated. The data of 21 MeV are almost perfectly described by Coulomb excitation calculations, as expected for this bombarding energy, because of the smaller nuclear interaction in this energy range (below the Coulomb barrier). For 24 and 27 MeV the back angle data are well described by the CRC-1n calculations, which, in principle, is the most complete and reliable one.

It seems unlikely that the inclusion of additional channels would improve significantly the agreement with the experimental large angle cross sections (especially for the region of the last experimental point 24 MeV) since, as has been discussed, their coupling tends to

decrease somewhat the angular distribution for large angles. The existing discrepancies between theoretical calculations and data might be connected with possible uncertainties in the optical potentials, or in the treatment the break-up and other reaction processes (the ^{121}Sn nucleus, for example, has an excited state of only 6 keV, implying that the subsequent 2n transfer could occur by this state and not only by the ^{121}Sn ground state).

It is remarkable how the coupling of transfer channels changes in a more significant way the elastic channel rather than the inelastic one (when comparing CC+PP with CRC-1n+PP). The interpretation of these results requires additional theoretical studies. Further data should be measured at additional energies (particularly near the barrier) and with a larger density of data points, both in this and other similar systems in order to adequately investigate this effect. It is also important to say that the non inclusion of the TELP does not change the calculated inelastic angular distributions significantly (and the total reaction cross section has less than 5% difference).

6. Conclusions

The measurement of γ-particle coincidences using the Saci–Perere γ-ray spectrometer (LAFN-IFUSP-DFN) was performed and the angular distribution for the 2^+ excited state of ^{120}Sn was obtained at 21, 24 and 27 MeV. These measurements contribute to consolidate the experimental method originally developed with the study of ^{18}O + ^{110}Pd inelastic scattering.

Extensive calculations were performed allowing for the comparison of different theoretical models for the reaction mechanisms. The effect of break-up was included in the calculations via the introduction of a polarization potential (obtained from CDCC calculations). Its inclusion has little influence on the description of the experimental data. The elastic scattering data, previously available from [6], turned out to be inconsistent with the 2n stripping direct transfer model. The analysis of the 2n transfer data can give a final indication if the process is sequential or direct.

The small differences existing between calculations and inelastic data might be due to the chosen potential or to the adopted break-up and other reaction process models used. The coupling of transfer reactions changes the elastic channel much more than the inelastic one.

In this experiment the break-up of the ejectiles after transfers was also observed (both in 1p pickup and 2n stripping). The analysis of these channels is under way and the results should be submitted for publication soon. Also the single neutron stripping channel was observed. Additional measurements would be useful to further investigate this and other systems, as discussed in the previous section. We plan to build a new detector setup with much higher granularity and angular coverage in the near future for this type of measurement.

Acknowledgments

This work was partially supported by FAPESP, CAPES and CNPq, Brazil.

References

[1] Alcántara-Núñez J A, Oliveira J R B *et al* 2003 *Nucl. Inst. Meth.* A **497** 429
[2] Zagatto V A B, de Oliveira J R B *et al* 2014 *Nucl. Inst. Meth.* A **749** 19–26
[3] Martinez Heimann D, Pacheco A J, Capurro O A, Arazi A, Carnelli P F F *et al* 2012 *AIP Conf. Proc.* **1423** 109

[4] Shrivastava A, Navin A, Keeley N, Mahata K, Ramachandran K, Nanal V, Parkar V V, Chater-jee A and Kailas S 2006 *Phys. Lett.* B **633** 463–8
[5] Becker K, Blatt K, Jansch H J, Korsch W, Leucker H, Luck W, Reich H, Volk H-G and Fick D 1991 *Nucl. Phys.* A **535** 189–202
[6] Sousa D P *et al* 2010 *Nucl. Phy.* A **836** 1–0
[7] Sousa D P 2008 *Master's Dissertation* Universidade de São Paulo (http://teses.usp.br/teses/disponiveis/43/43134/tde-28082008-142110/pt-br.php)
[8] Davis N J *et al* 2004 *Phys. Rev.* C **69** 064605
[9] Tokimoto Y, Utsunomiya H, Yamagata T, Ohta M, Lui Y-W, Schmitt R P, Typel S, Aoki Y, Ieki K and Katori K 2001 *Phys. Rev.* C **63** 035801
[10] Luong D H, Dasgupta M, Hinde D J, du Rietz R, Rafiei R, Lin C J, Evers M and Diaz-Torres A 2011 *Phys. Lett.* B **695** 105–9
[11] Zagatto V A B 2011 *Master's Dissertation* Universidade de São Paulo (http://teses.usp.br/teses/disponiveis/43/43134/tde-26042012-195616/pt-br.php)
[12] Thompson I J 1988 *Comp. Phys. Rep.* **7** 167
[13] Diaz-Torres A, Thompsom I J and Beck C 2003 *Phys. Rev.* C **68** 044607
[14] Thompson I J, Nagarajan M A, Lilley J S and Smithson M J 1989 *Nucl. Phys.* A **505** 84
[15] Broglia R A and Winther A 1991 *Heavy-Ion Reactions*Parts *I and II FIP Lecture Notes Series* (New York: Addison-Wesley)
[16] Diaz-Torres A and Thompson I J 2002 *Phys. Rev.* C **65** 024606
[17] Brink D M 1972 *Phys. Lett.* B **40** 37
[18] Broglia R A and Winther A 1972 *Phys. Rep.* **4** 153
[19] Thompson I J 2011 Fresco Manual *Version FRES* **2.9** 14–6 (http://fresco.org.uk/documentation.htm)
[20] 2015 (http://nndc.bnl.gov/useroutput/AR2261B9DE494815AD0A35B061595CABC51.html)
[21] Cândido Ribeiro M A, Chamon L C, Pereira D, Hussein M S and Galleti D 1997 *Phys. Rev. Lett.* **78** 3270
[22] Chamon L C, Pereira D, Hussein M S, Ribeiro M A C and Galleti D 1997 *Phys. Rev. Lett.* **70** 5218
[23] Chamon L C *et al* 2002 *Phys. Rev.* C **66** 014610
[24] Udagawa T, Wolter H H and Coker W R 1973 *Phys. Rev. Letts.* **31** 1507
[25] Czosnyka T, Cline D and Wu C Y 1983 *Bull. Amer. Phys. Soc.* **28** 745